DEEP-Theory Meeting   9 Jan 2017

RECENT PROGRESS ON LARGE-SCALE STRUCTURE

DM halo properties vs. density paper in press; **halo stripping** and **halo radial profile** papers being drafted (with Christoph Lee, Doug Hellinger).

AAS Poster by Tze Goh showing halo properties like concentration, accretion history, and spin are mainly determined by environmental density rather than by location within the cosmic web. The poster compared properties vs. environmental density in cosmic walls and all web locations, and found few differences. (with Tze Goh, Christoph Lee, Peter Behroozi, Doug Hellinger, Miguel Aragon Calvo)

Galaxy R_{eff} predicted by (spin parameter)(halo radius) paper led by Rachel Somerville in nearly final form at https://www.dropbox.com/s/theqlr7ql22kfio/rgrh.pdf?dl=0

Galaxy Stochastic Order Redshift Technique (SORT): a simple, efficient, and robust method to improve cosmological photometric redshift measurements, by Nicholas Tejos, Aldo Rodriguez-Puebla, and Joel (submitted to MNRAS)

Constraining the Galaxy Halo Connection: Star Formation Histories, Galaxy Mergers, and Structural Properties, by Aldo Rodriguez-Puebla, Joel, and others (in nearly final form)

Abundance Matching is Independent of Cosmic Environment Density, based on Radu Dragomir's UCSC senior thesis, advised by Aldo and Joel (we're drafting this now)

Two UCSC astrophysics students working with us received **Koret Undergraduate Research Scholarships**: **Elliot Eckhard**, who is help visualize large scale structure, and **Sean Larkin**, who is working on the Deep Learning project

AAS Poster by Tze Goh showing halo properties like concentration, accretion history, and spin are mainly determined by environmental density rather than by location within the cosmic web. Download the poster at http://spineoftheweb.blogspot.com/

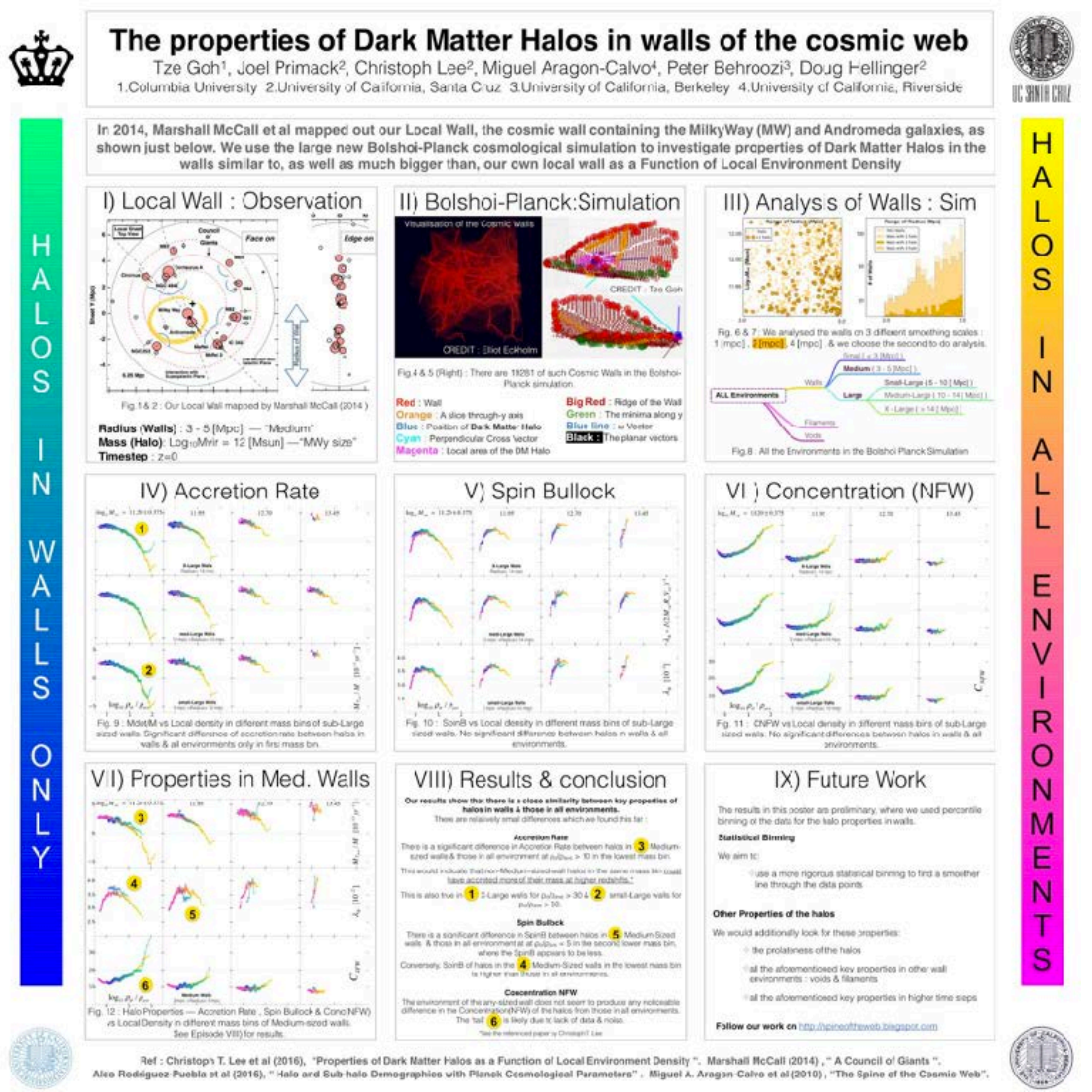

The Relationship between Galaxy and Dark Matter Halo Size from $z \sim 3$ to the present

Rachel S. Somerville[1,2], Peter Behroozi[3], Viraj Pandya[4], Avishai Dekel[5], S. M. Faber[4], H. C. Ferguson[6], Adriano Fontana[10], Kuang-Han Huang[7], Anton M. Koekemoer[6], David Koo[4], P. G. Pérez-González[8], Joel R. Primack[9], Paola Santini[10], Edward N. Taylor[11], Arjen van der Wel[12]

paper led by Rachel Somerville in nearly final form at https://www.dropbox.com/s/theqlr7ql22kfio/rgrh.pdf?dl=0 on which Rachel requested comments by Jan 3

$$\mathrm{SHRH}\lambda \equiv R_{\mathrm{eff}}/(\lambda\, R_{\mathrm{halo}})$$

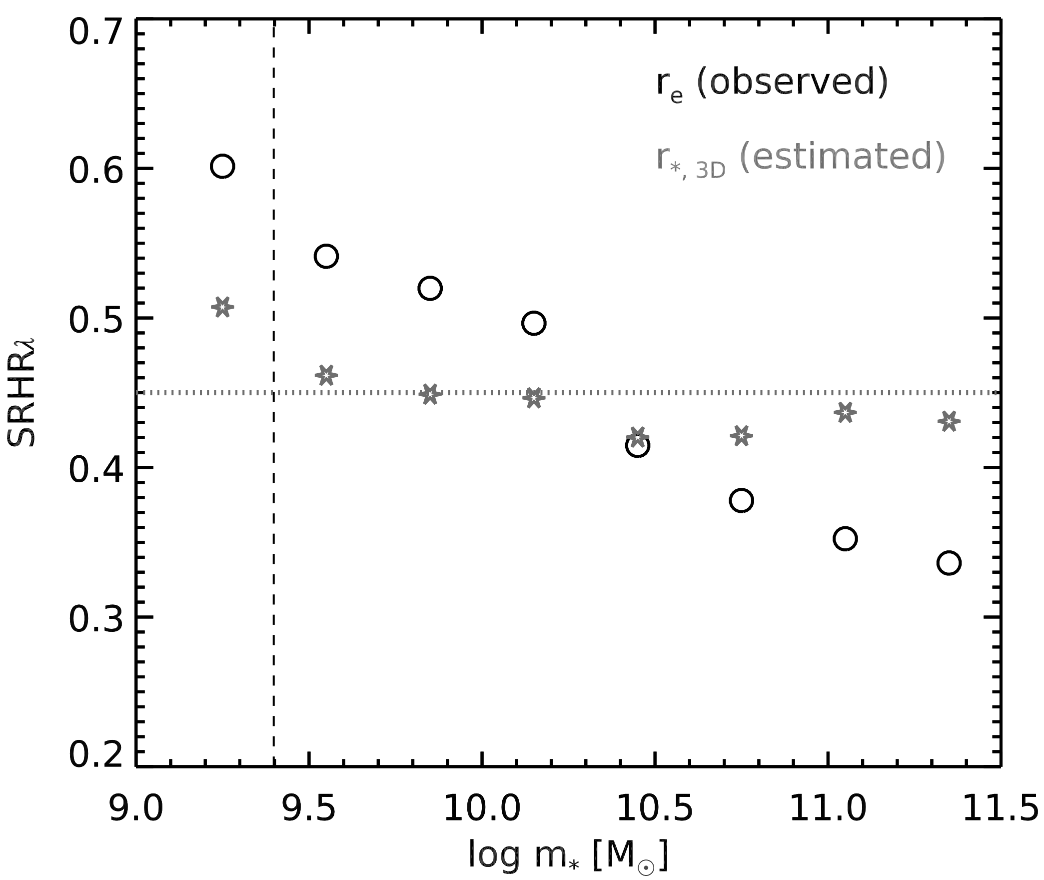

Figure 5. Median radius divided by the median value of the spin parameter times the halo virial radius, in bins of stellar mass, at $z \sim 0.1$. Open circles are based on the GAMA DR2 catalogs and are for the observed (projected) r-band half-light radius r_e. **The dashed vertical line shows the 97.7% stellar mass completeness limit for the GAMA sample.** Gray star symbols show the same quantity for the estimated 3D half-stellar mass radius ($r_{*,3D}$). It is striking that the ratio between galaxy size and halo size remains so nearly constant over a wide range in stellar mass.

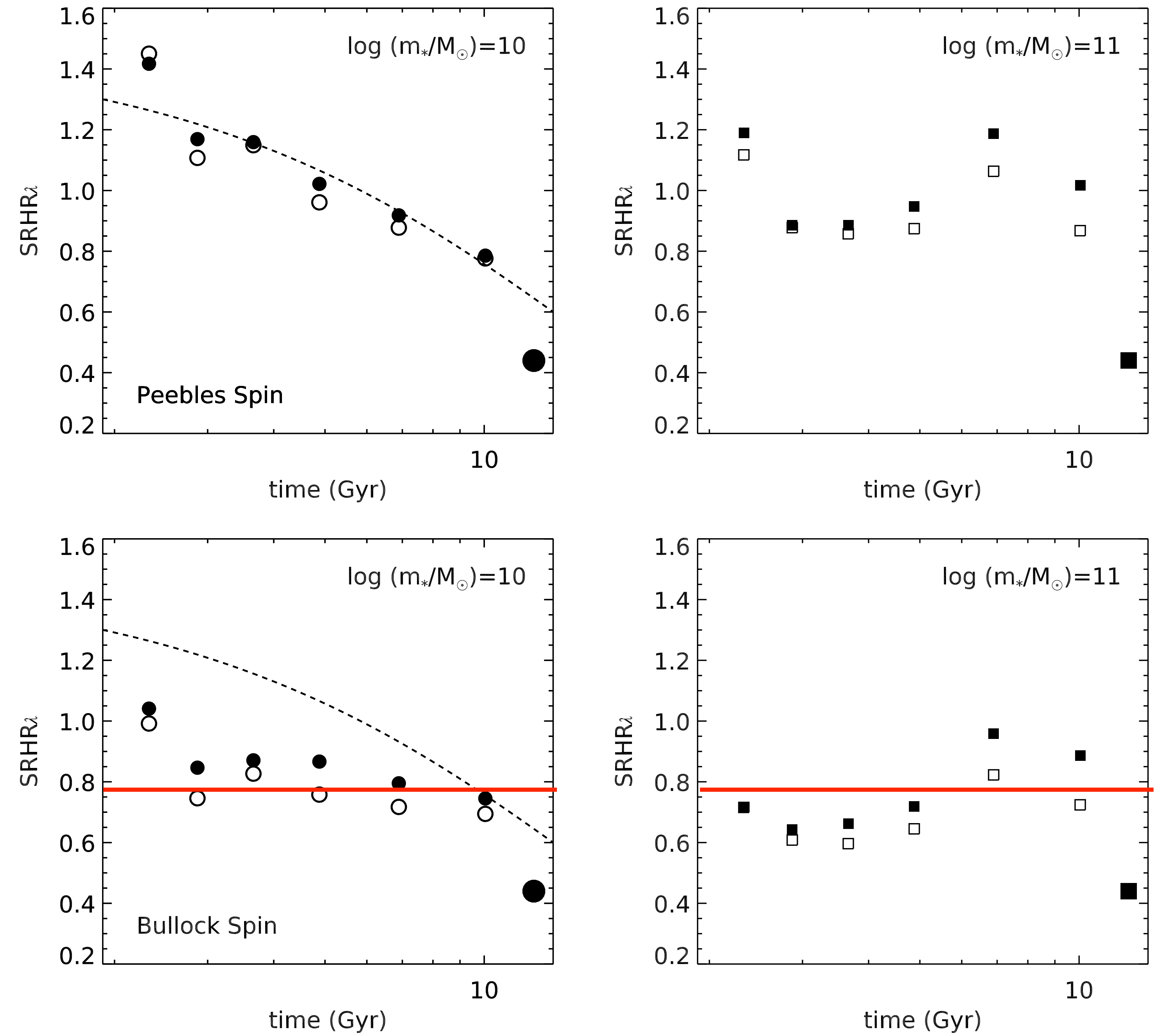

Figure 9. Time evolution of the ratio between median $r_{*,3D}$ and λR_h for two different stellar mass bins: $10^{9.75}\,\mathrm{M}_\odot < m_* < 10^{10.25}\,\mathrm{M}_\odot$ (left; filled) and $10^{10.75}\,\mathrm{M}_\odot < m_* < 10^{11.25}\,\mathrm{M}_\odot$ (right; filled). Top row: Peebles spin; Bottom row: Bullock spin. The result for the $z = 0.1$ GAMA sample is nearly identical for both mass bins, and is shown by the large symbol. The ratio of the mean quantities is shown by the open symbols — using means instead of medians results in slightly different values of SRHRλ, but does not change any of the trends. The time dependence of SRHRλ for the lower stellar mass bins (when using the Peebles spin) is fairly well fit by a declining exponential with a timescale of 15 Gyr (shown by the dashed line in both of the left panels). The value of SRHRλ for massive galaxies remains nearly constant, or increases slightly, with cosmic time within the CANDELS sample. The CANDELS values, however, seem systematically higher than those derived for GAMA.

DEEP-Theory Meeting   9 Jan 2017

RECENT PROGRESS ON GALAXY FORMATION

Progress generating mock images and IFU data cubes from our Sunrise pipeline (Greg Snyder, Raymond Simons) Email 1/8 from Greg: I am pleased to report that I have finished creating Sunrise images on the entire suite of VELA Generation 3 simulations. There were 34 simulations that had enough snapshots to consider. I have copied them all to Pleiades and applied Raymond's speedy yt->Sunrise extraction algorithm and our Sunrise imaging pipeline. I am finished with Candelizing 75% of the sample and I expect to reach 100% by later this week, at which point I will copy out these files. One new improvement is that I have added filters for JWST's MIRI instrument in addition to NIRCAM and HST for the set of candelized images. MIRI (5-25 microns) will only make sense for the higher redshifts because we didn't do dust emission, but could help characterize shapes in the very early universe.

I have not yet done a thorough investigation to make sure each snapshot looks OK. In particular, our choice of image field of view may have to be adjusted bigger or smaller on a case by case basis as we start looking at them. Everything is fully automated and debugged so it wouldn't take long to redo any needing this adjustment.

Analyzing these images for **clumps** (Yicheng Guo); measuring **GALFIT statistics** a, b, axis ratio b/a, Sersic index of CANDELized images (Yicheng and Vivian Tang) compared with high resolution images (Liz McGrath). **R_{eff} for SDSS galaxies as a function of density** (Christoph, Graham Vanbenthuysen).

Preparing information for deep learning (DL) about the simulations using yt analysis of the saved timesteps (Sean Larkin, Fernando Caro, Christoph Lee) and using other methods (Nir Mandelker, Santi Roca-Fabrega) to see **whether giving the deep learning code this information in addition to mock images will allow the code to determine some of these phenomena from the images** at least in the best cases of inclination, resolution, and signal/noise (Marc Huertas-Company and team). **What data about the simulations should we give DL? Can we make sufficient progress by HST Cycle 24 deadline April 8?**

Stochastic Order Redshift Technique (SORT): a simple, efficient and robust method to improve cosmological redshift measurements

Nicolas Tejos, Aldo Rodríguez-Puebla and Joel R. Primack (submitted to MNRAS)

ABSTRACT

We present a simple, efficient and robust approach to improve cosmological redshift measurements. The method is based on the presence of a reference sample for which a precise redshift number distribution (dN/dz) can be obtained for different pencil-beam-like sub-volumes within the original survey. For each sub-volume we then impose: (i) that the redshift number distribution of the uncertain redshift measurements matches the reference dN/dz corrected by their selection functions; and (ii) the rank order in redshift of the original ensemble of uncertain measurements is preserved. The latter step is motivated by the fact that random variables drawn from Gaussian probability density functions (PDFs) of different means and arbitrarily large standard deviations satisfy stochastic ordering. We then repeat this simple algorithm for multiple arbitrary pencil-beam-like overlapping sub-volumes; in this manner, each uncertain measurement has multiple (non-independent) "recovered" redshifts which can be used to estimate a new redshift PDF. We refer to this method as the Stochastic Order Redshift Technique (SORT). We have used a state-of-the art N-body simulation to test the performance of SORT under simple assumptions and found that it can improve the quality of cosmological redshifts in an robust and efficient manner. Particularly, SORT redshifts ($z_{\rm sort}$) are able to recover the distinctive features of the so-called 'cosmic web' and can provide unbiased measurement of the two-point correlation function on scales $\gtrsim 4\,h^{-1}$Mpc. Given its simplicity, we envision that a method like SORT can be incorporated into more sophisticated algorithms aimed to exploit the full potential of large extragalactic photometric surveys.

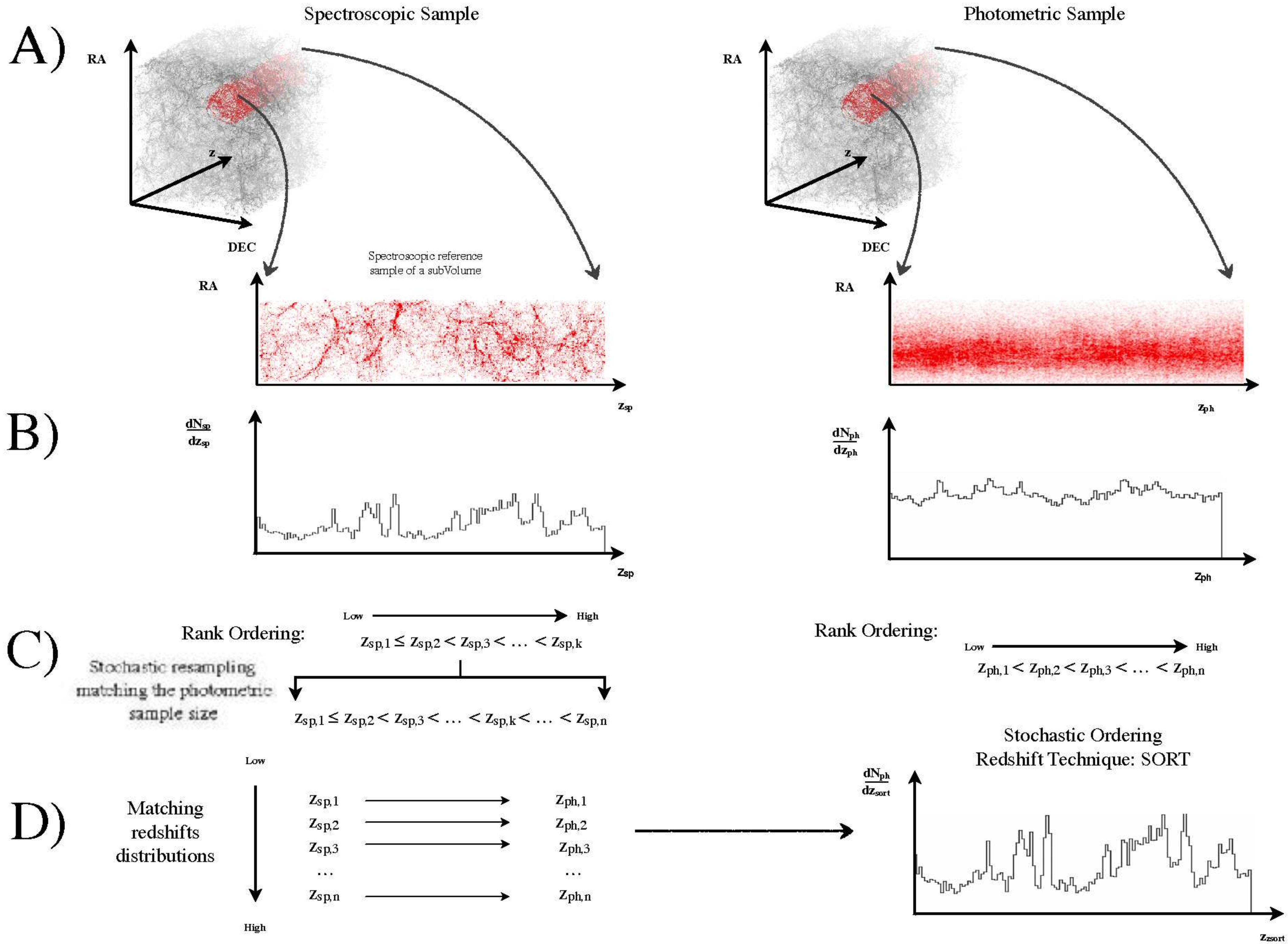

Figure 1. An illustration of our method based on stochastic order. *Step (A):* In a given pencil-beam-like sub-volume we define two samples of extragalactic objects depending on the accuracy of their cosmological redshift determination: precise (e.g. spectroscopic; left panels) and uncertain (e.g. photometric; right panels). *Step (B):* From both samples we observe a redshift number density, dN/dz. In principle, the uncertain dN/dz (left panel) is a *nosier* version of the precise one (right panel). *Step (C):* From the precise distribution we create a new re-sampled redshift distribution matching the number of objects in the uncertain sample (left panel) and sort it from low to high redshift. We also sort the observed uncertain redshift distribution from low to high redshift (right panel). *Step (D):* Finally, we perform a one-to-one match between the recovered distribution in the left and right panels of step (C). We refer to this simple algorithm as Stochastic Ordering Redshift Technique (SORT).

Galaxy Stochastic Order Redshift Technique (SORT): a simple, efficient, and robust method to improve cosmological photometric redshift measurements

METHOD DETAILS

(i) For each individual galaxy with apparent magnitude m, we define a projected area A as a circle of angular radius R.

(ii) We then consider only galaxies in A having apparent magnitudes within Δm from m.

(iii) From these galaxies, we check that at least $N_{\rm min}^{\rm ref}$ have spectroscopic redshifts. Otherwise, we iterate steps (i) and (ii) increasing the values of R and Δm by δR and δm, respectively, until the condition is satisfied.

(iv) We compute a redshift histogram of the $N^{\rm ref}$ galaxies using redshift bins of width $\delta z/3$. We then convolve this histogram with a Gaussian kernel of standard deviation δz, and use the resulting distribution to randomly sample $N_{\rm ph}^{\rm rec}$ redshifts, where $N_{\rm ph}^{\rm rec}$ is the number of photometric galaxies within A.

(v) We apply the stochastic order matching scheme described in Section 2.2 (see Equation (8)) to obtain *recovered* redshifts for each individual photometric galaxy.

We solve Equation (7) by sorting the $N_{\rm ph}$ *observed* photometric redshifts such that $z_1^{\rm obs} \leqslant z_2^{\rm obs} \leqslant \ldots \leqslant z_{N_{\rm ph}}^{\rm obs}$, and assign them $N_{\rm ph}$ sorted *recovered* redshifts, randomly sampled from,

$$\frac{N_{\rm ph}}{N_{\rm sp}} \frac{S_{\rm ph}}{S_{\rm sp}} \frac{dN_{\rm sp}}{dz}(z) \rightarrow \{z_1^{\rm rec}, z_2^{\rm rec}, \ldots, z_{N_{\rm ph}}^{\rm rec}\} \qquad (8)$$

such that $z_1^{\rm rec} \leqslant z_2^{\rm rec} \leqslant \ldots \leqslant z_{N_{\rm ph}}^{\rm rec}$. This provides a straightforward one-to-one mapping between the observed and *recovered* photometric redshift distributions as $z_i^{\rm obs} \leftrightarrow z_i^{\rm rec}$, for $i \in \{1, 2, \ldots, N_{\rm ph}\}$ (see bottom panel of Figure 1). This is a simplistic but powerful approach, particularly because photometric samples are expected to satisfy *stochastic ordering*.

We repeated this algorithm for *all* the photometric galaxies in the sample. In this manner, each photometric galaxy has a *list* of recovered redshifts, each one coming from an independent random sampling of their respective reference (spectroscopic) sample. This is equivalent to having *adaptive* Monte Carlo realizations, as galaxies in denser regions will be sampled more times than galaxies in less dense regions. For simplicity, we finally take the median value of the aforementioned recovered distribution list as the actual unique *recovered* SORT redshift, $z_{\rm sort}$.

For the results of this paper we applied the aforementioned algorithm using the following parameters: $R = 1$ degree, $\Delta m = 0.2$ mag, $\delta R = 0.1$ degree, $\delta m = 0.1$ mag, $N_{\rm min}^{\rm ref} = 2$ and $\delta z = 0.0003$. By choosing $N_{\rm min}^{\rm ref} = 2$ we make sure that for each iteration there are at least 2 galaxies with a spectroscopic redshift measurement as reference. Because of our survey is magnitude limited, for the brightest galaxies this condition means that the radius of the search ends up being larger than the fiducial value $R = 1$ degree, up to a factor of $\approx 1.5 - 2.5\times$ for those with magnitudes $m \sim 15 - 14$ mag respectively. The fraction of bright galaxies is very small and we do not consider this issue to be a major limitation of our method; in any case, the brightest objects are the cheapest to get a spectroscopic redshift for, hence making it feasible to eventually correct for this in the future.

We have chosen a relatively small $\Delta m = 0.2$ mag in order to ensure a similar selection function for galaxies for the photometric and spectroscopic samples as a function of m. In this manner we avoid introducing shot noise from correcting for the different selection functions with a sparse sampling.

Galaxy Stochastic Order Redshift Technique (SORT): a simple, efficient, and robust method to improve cosmological photometric redshift measurements, by Nicholas Tejos, Aldo Rodriguez-Puebla, and Joel (submitted to MNRAS)

To test the method we created a sample of dark matter halos in redshift space from the MultiDark-Planck simulation using

$$1 + z_{\rm true} = (1 + z_{\rm cos})(1 + \frac{\Delta v_{\rm los}}{c})$$

and then added noise to simulate observed redshifts, with $\sigma^{ph} = 0.02$ (70%) and $\sigma^{spect} = 0.0001$ (30%)

$$z_{\rm obs} = z_{\rm true} + \delta_z(1 + z_{\rm true})$$

Our sample consisted of 127993 dark matter halos, which we think of as being from SDSS at z ~ 0.15, but we also experimented with much larger σ^{ph} and smaller spectroscopic fractions. Results for this first test:

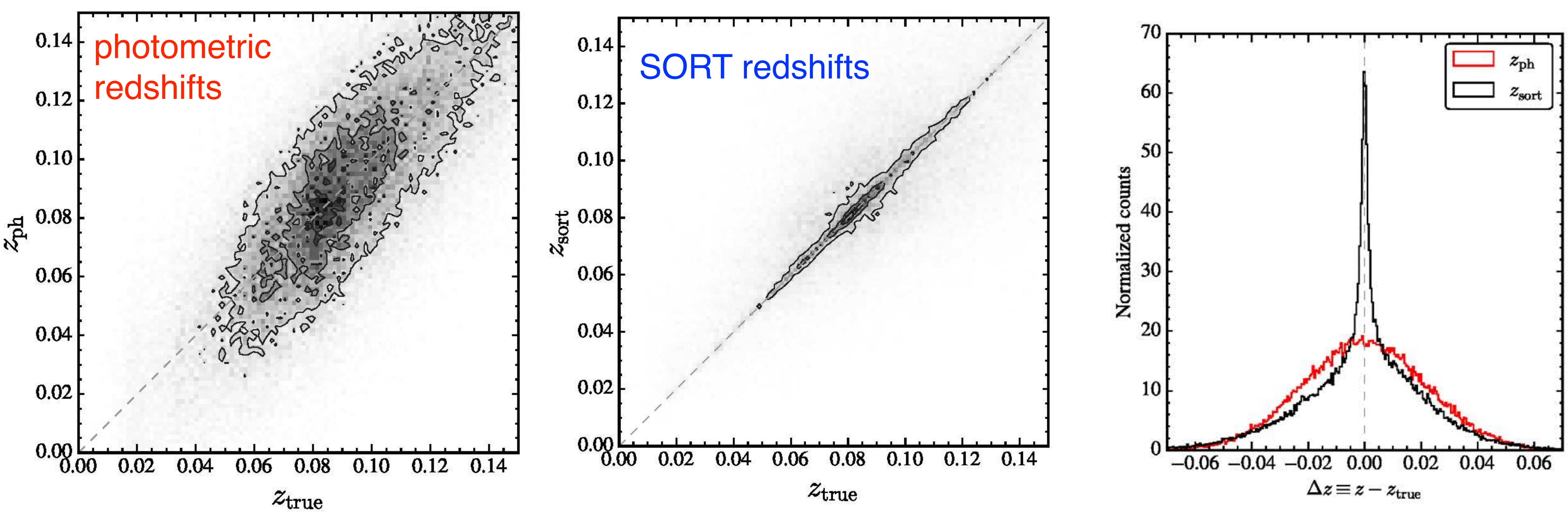

SORT allows recovery of the 2-point correlation function for *s* > 4 Mpc/h

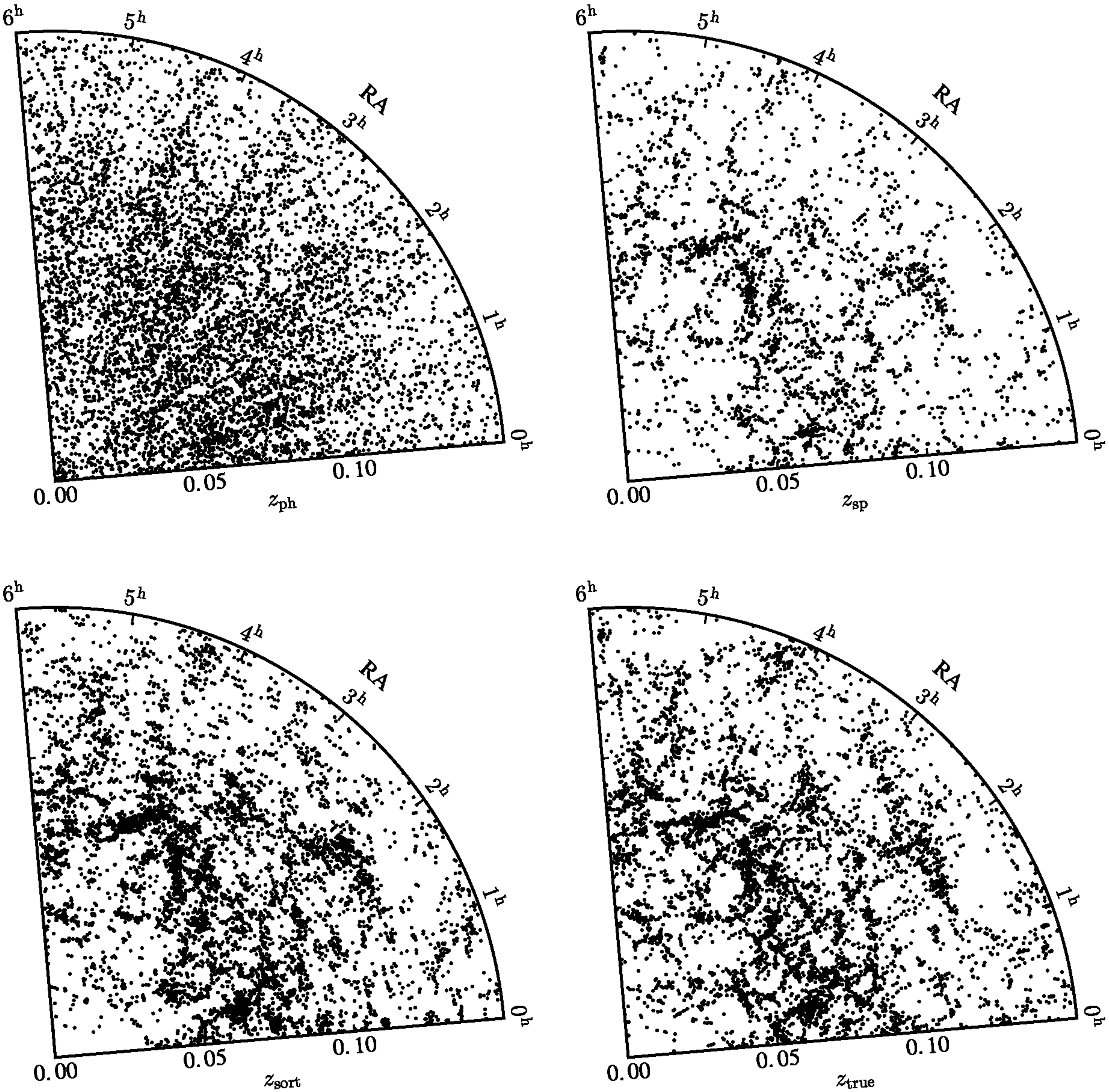

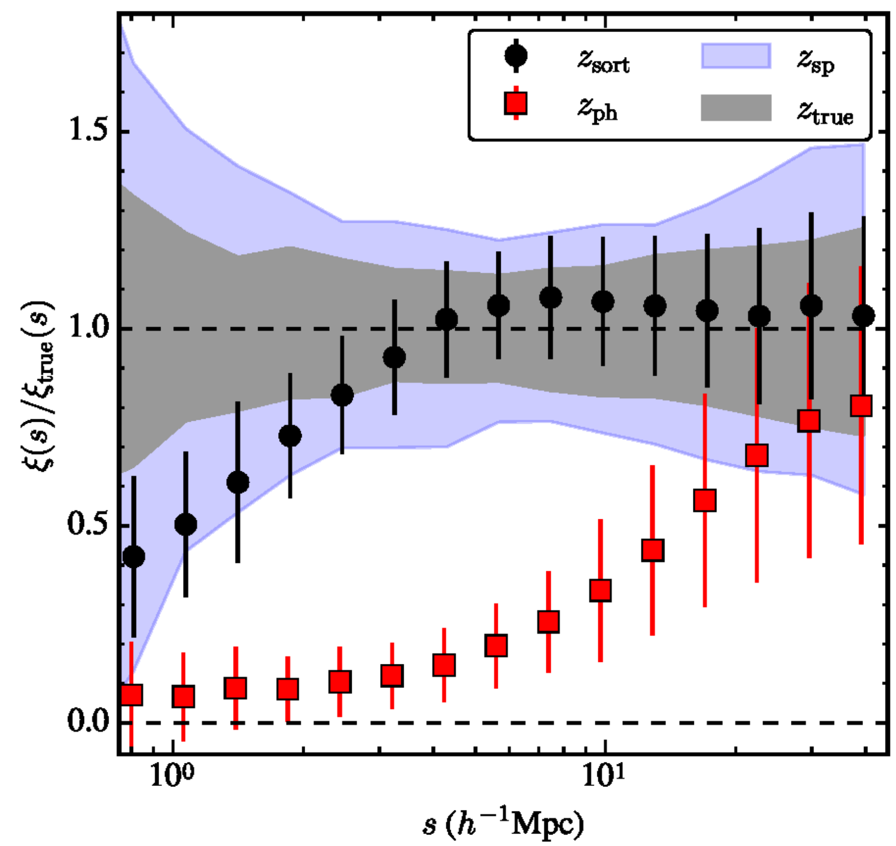

Figure 7. The ratio between the measured redshift-space two-point correlation function and its underlying true value, $\xi(s)/\xi_{\rm true}(s)$, as a function of redshift space distance s. The black circles correspond to using $z_{\rm sort}$ and the red squares correspond to using $z_{\rm ph}$ (slightly offset in the x-axis for clarity). Uncertainties were estimated from a bootstrap technique from 100 realizations. The grey shaded area corresponds to the intrinsic 1σ uncertainty limit due to sample variance (i.e. this is the uncertainty assuming we knew the underlying true redshift for all the galaxies in the original photometric sample). The light-blue area corresponds to the 1σ uncertainty around the unbiased $z_{\rm sp}$ measurement from the spectroscopic sample (i.e. the remaining 30% of galaxies used as reference). See Section 4.3.2 for further details.

SORT works pretty well with much smaller fractions of spectroscopic redshifts (left panel) and much larger photometric redshift uncertainties (right panel)

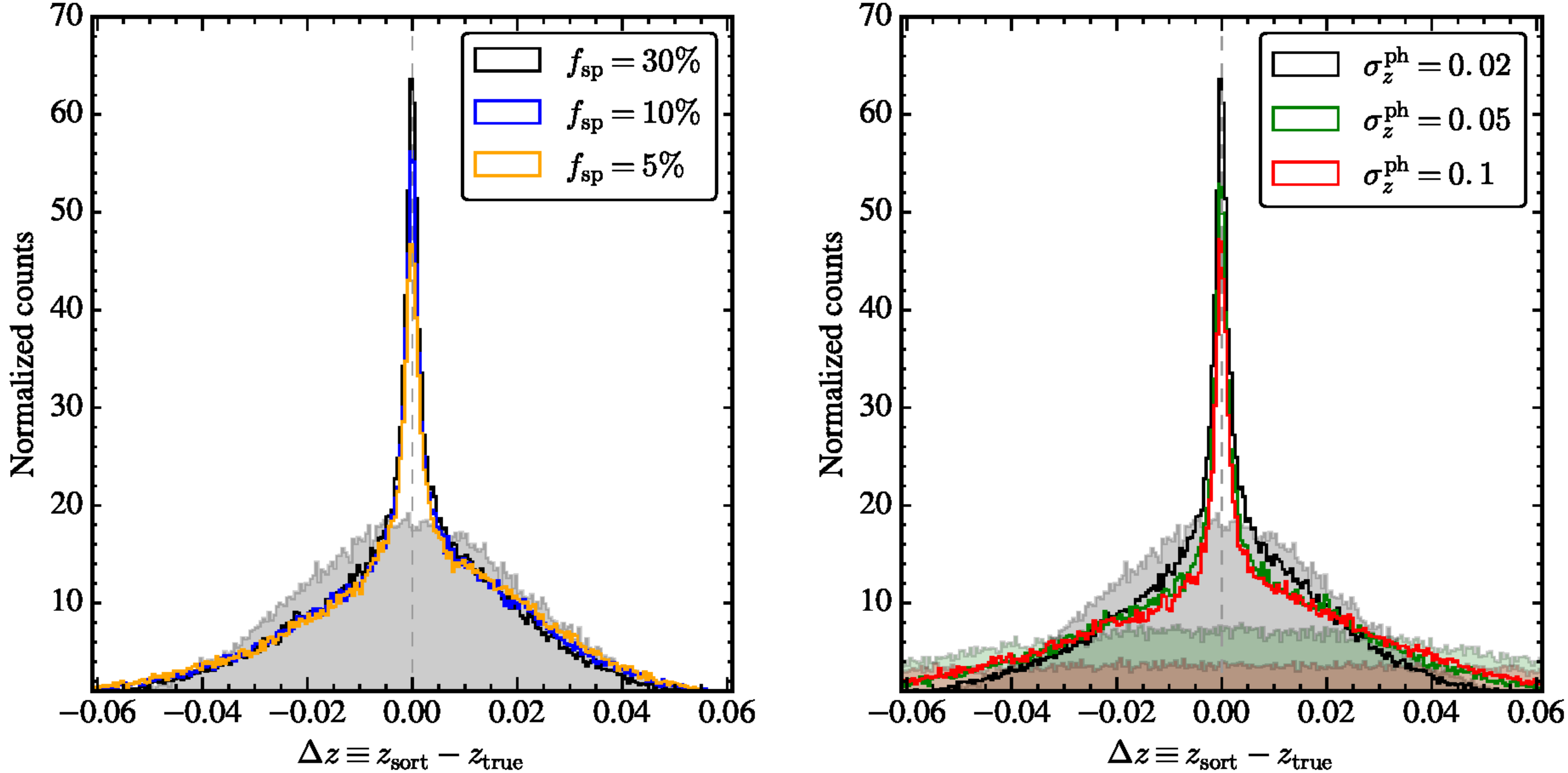

Figure 9. *Left panel:* redshift difference $\Delta z \equiv z_{\rm sort} - z_{\rm true}$ using different percentages of galaxies as reference (spectroscopic): $f_{\rm sp} = 30\%$ (our fiducial value; black histogram), $f_{\rm sp} = 10\%$ (blue histogram) and $f_{\rm sp} = 5\%$ (orange histogram). As reference, the original $\Delta z = z_{\rm ph} - z_{\rm true}$ distribution is shown as a shaded grey. *Right panel:* redshift difference $\Delta z \equiv z_{\rm sort} - z_{\rm true}$ using different values for the original redshift uncertainties: $\sigma_z^{\rm ph} = 0.02$ (our fiducial value; black histogram), $\sigma_z^{\rm ph} = 0.05$ (green histogram) and $\sigma_z^{\rm ph} = 0.1$ (red histogram). As reference, the original $\Delta z = z_{\rm ph} - z_{\rm true}$ distributions are shown as the shaded grey, light-green and light-red histograms, respectively. See Section 5.2 for further details.

Constraining the Galaxy Halo Connection: Star Formation Histories, Galaxy Mergers, and Structural Properties, by Aldo Rodriguez-Puebla, Joel, and others (in nearly final form) PREVIEW

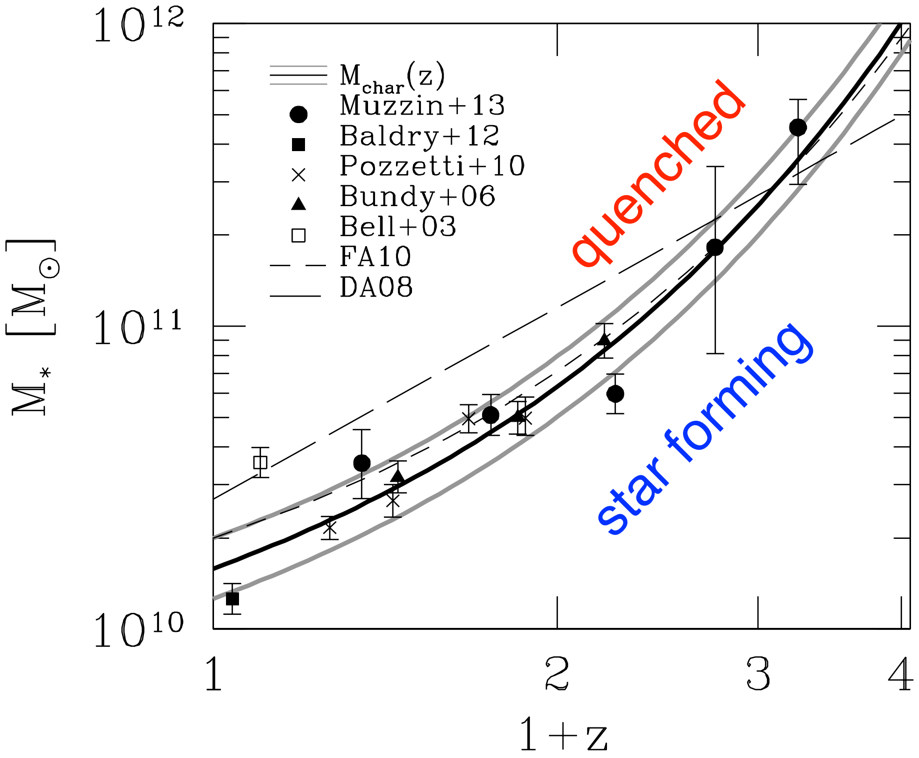

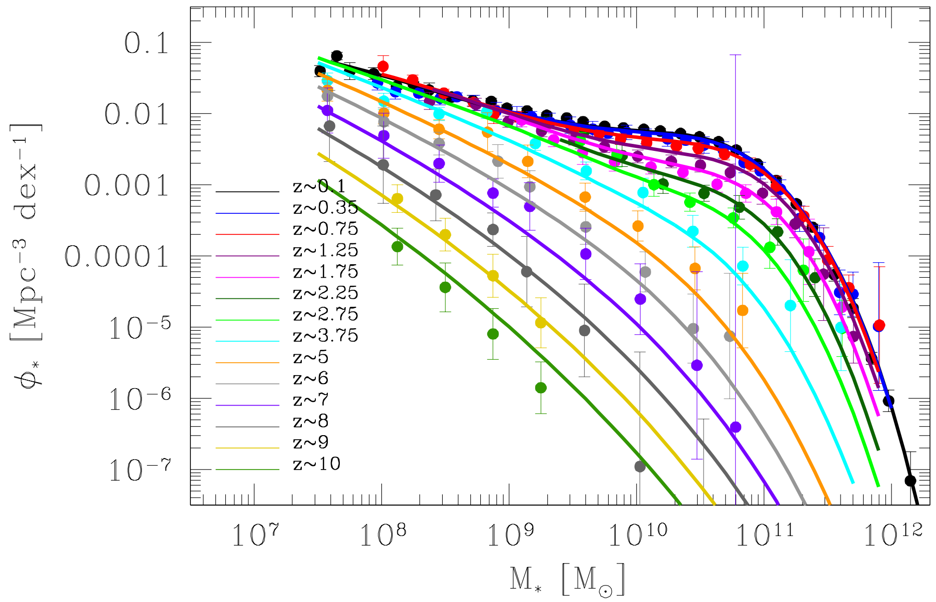

Figure 2. Redshift evolution from $z \sim 0.1$ to $z \sim 10$ of the galaxy stellar mass function (GSMF) derived by using 22 observational samples from the literature and represented with the filled circles with error bars. The various GSMFs have been corrected for potential systematics that could affect our results, see the text for details. Solid lines are the best fit model from a set of 5×10^5 MCMC models. These fits take into account uncertainties affecting the GSMF as discussed in the text. Note that at lower redshifts ($z \lesssim 3$) galaxies tend to pile up at $M_* \sim 3 \times 10^{10} M_\odot$ due to the increase of massive quench galaxies at lower redshifts.

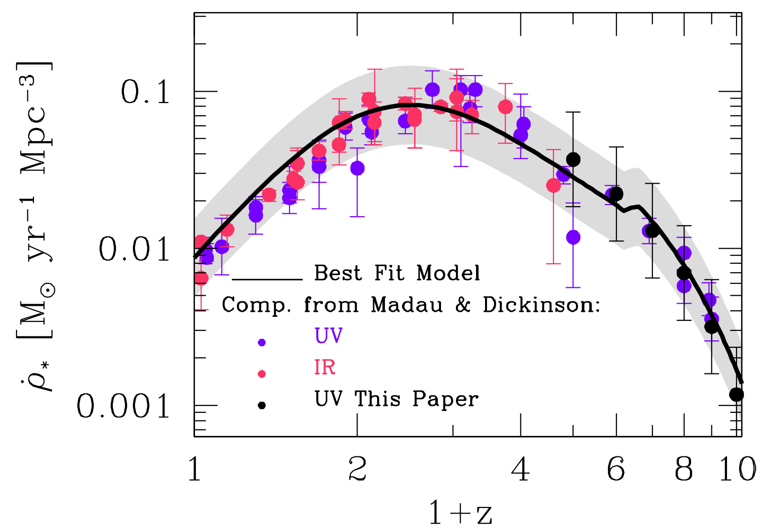

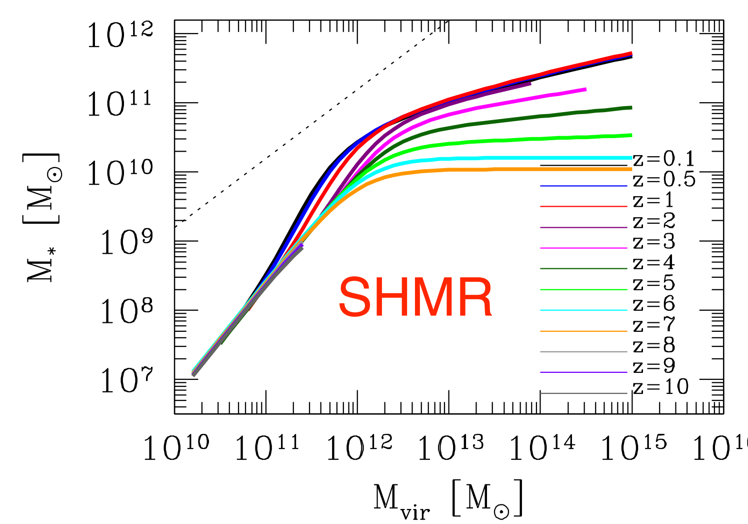

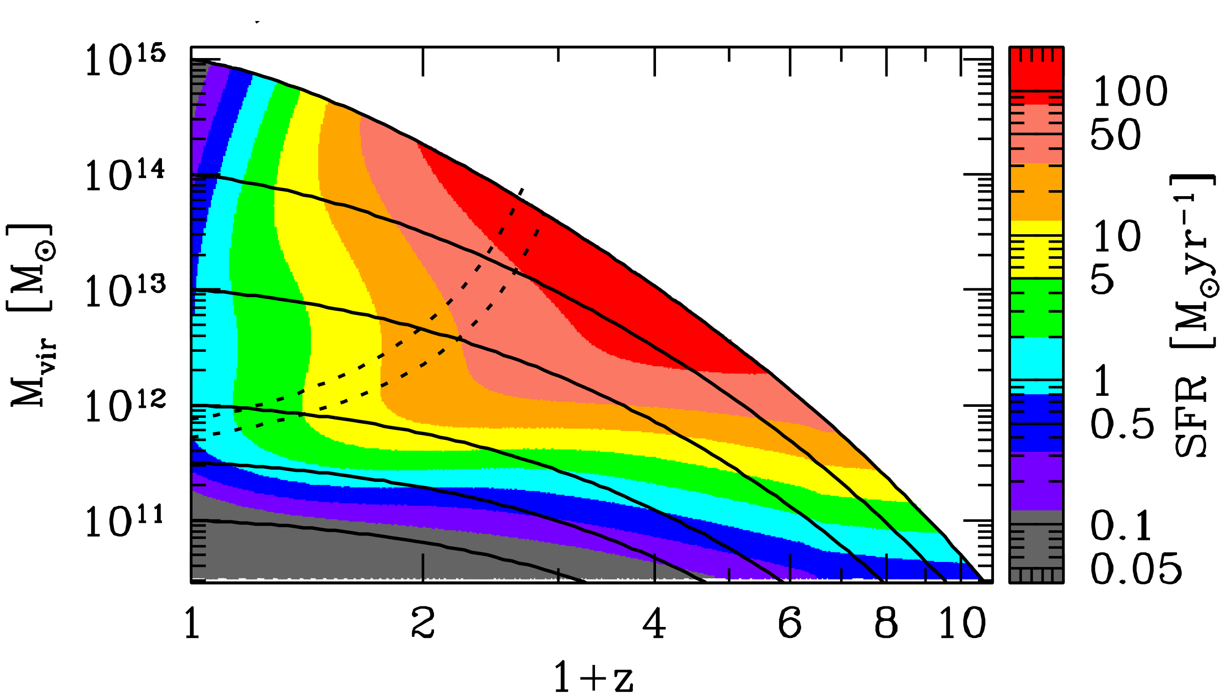

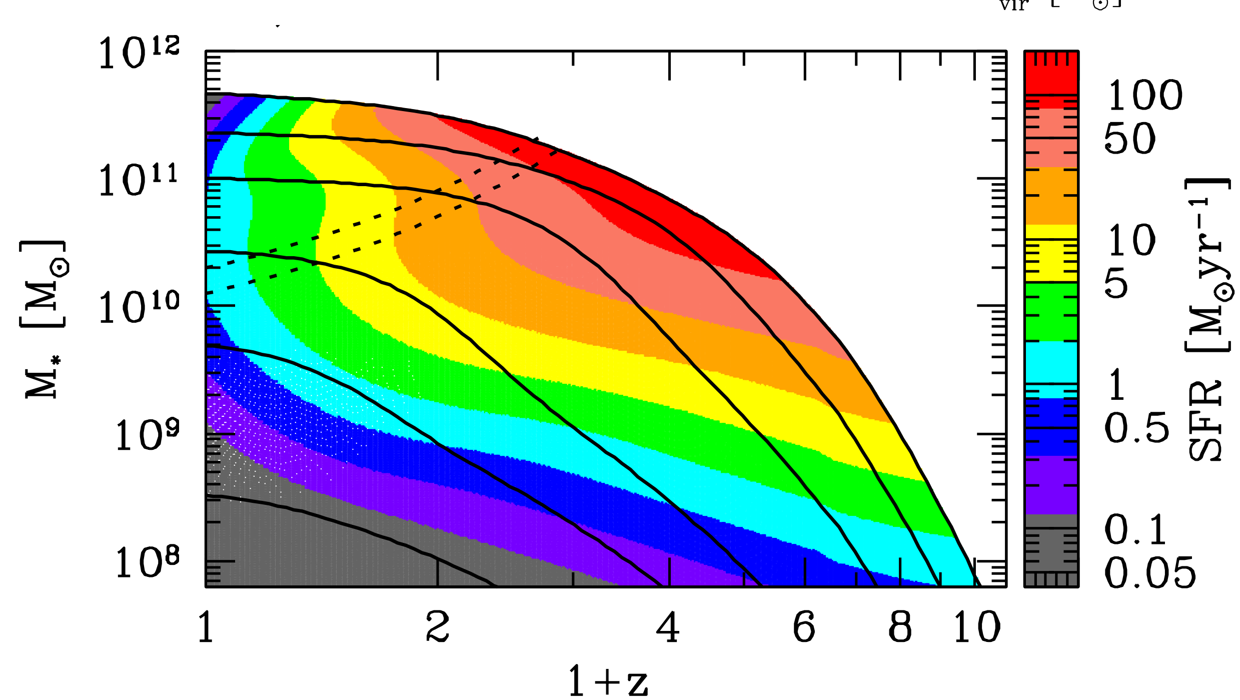

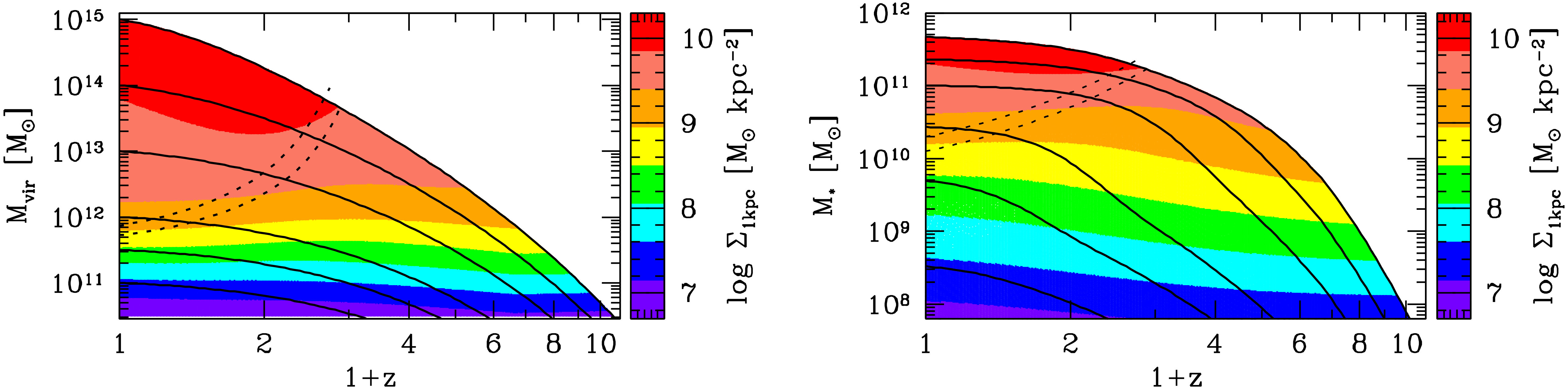

Figure 14. Integrated mass density at 1 kpc, as a function of halo mass (left panel) and stellar mass (right panel) for halo progenitors at $z = 0$. The black solid lines show the trajectories for progenitors with $M_{\rm vir} = 10^{11}, 10^{11.5}, 10^{12}, 10^{13}$, 10^{14} and $10^{15}\mathrm{M}_\odot$. The dotted line in the left hand panel shows the stellar mass and halo mass at which the observed fraction of star forming galaxies is equal to the quenched fraction of galaxies.

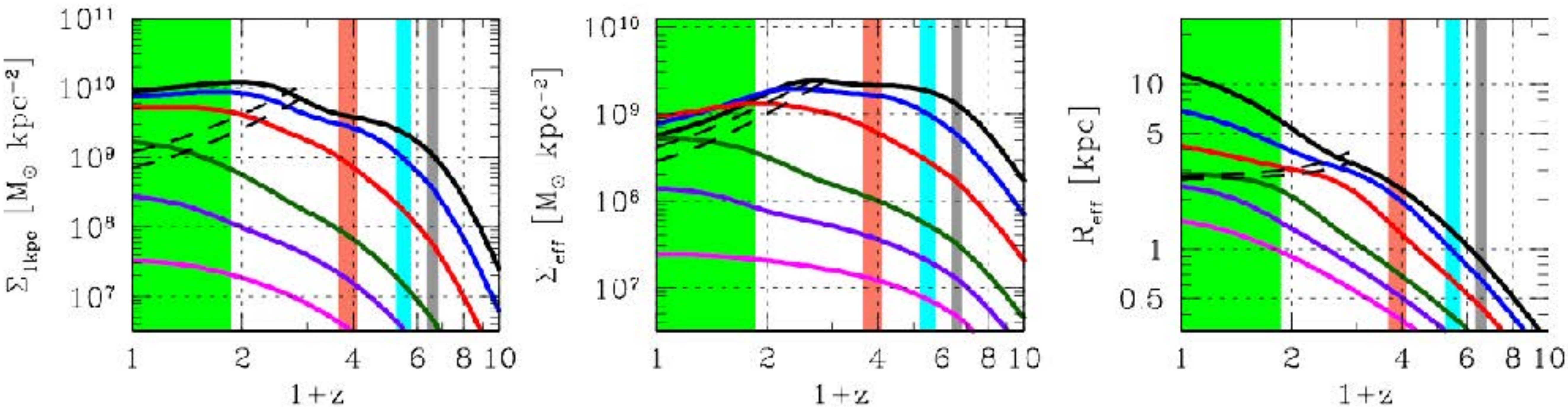

Figure 19. Summary plot for various galaxy properties: Panel a) Integrated surface mass density at 1 kpc, Panel b) Effective surface mass density and Panel c) Effective radius. The magenta, violet, green, red, blue and black lines show the trajectories for progenitors of $M_{vir} = 10^{11}$, $10^{11.5}$, 10^{12}, 10^{13}, 10^{14}, and $10^{15}M_\odot$. The gray, cyan, light red and light green shaded areas in all the panels show the epoch range at which the progenitors of halos of 10^{12}, 10^{13}, 10^{14}, and $10^{15}M_\odot$ reached the mass of $M_{vir} = 10^{11.8} - 10^{12}M_\odot$. The dashed lines show the transition when galaxies are statistically quenched. Note that the quenching transition occurs at $R_{eff} \approx 3$ kpc.